Graph-theoretic analysis of a model for the coupling between photosynthesis and photorespiration

Article *in* Canadian Journal of Chemistry · February 2014

DOI: 10.1139/cjc-2013-0315

2 authors:

Ruhul Amin
University of Alberta
11 PUBLICATIONS **46** CITATIONS
SEE PROFILE

Marc R Roussel
University of Lethbridge
86 PUBLICATIONS **2,105** CITATIONS
SEE PROFILE

Graph-Theoretic Analysis of a Model for the Coupling Between Photosynthesis and Photorespiration

Md. Ruhul Amin[1] and Marc R. Roussel[2]

Department of Chemistry and Biochemistry, University Hall, University of Lethbridge, Lethbridge, Alberta, T1K 3M4, Canada

[1]Current address: Department of Oncology, Cross Cancer Institute, University of Alberta

[2]Corresponding author (email: roussel@uleth.ca, phone: +1 403 329 2326, fax: +1 403 329 2057)

Graph-Theoretic Analysis of a Model for the Coupling Between Photosynthesis and Photorespiration

Md. Ruhul Amin and Marc R. Roussel

Abstract: We develop and analyze a mathematical model based on a previously enunciated hypothesis regarding the origin of rapid, irregular oscillations observed in photosynthetic variables when a leaf is transferred to a low CO_2 atmosphere. This model takes the form of a set of differential equations with two delays. We review graph-theoretical methods of analysis based on the bipartite graph representation of mass-action models, including models with delays. We illustrate the use of these methods by showing that our model is capable of delay-induced oscillations. We present some numerical examples confirming this possibility, including the possibility of complex transient oscillations. We then use the structure of the identified oscillophore, the part of the reaction network responsible for the oscillations, along with our knowledge of the plausible range of values for one of the delays to rule out this hypothetical mechanism.

Key words: delay-induced instability, graph-theoretical analysis, photosynthesis, photorespiration

Résumé: Nous présentons un modèle mathématique développé à partir d'une hypothèse récente sur l'origine d'oscillations rapides et irrégulières des variables photosynthétiques observées lorsqu'une feuille est introduite à une atmosphère à basse teneur en dioxyde de carbone. Ce modèle consiste d'un système d'équations différentielles avec deux retards.

Nous présentons brièvement des méthodes d'analyse de modèles à action de masse représentés par des graphes bipartis, y compris les modèles avec retards. Nous utilisons notre modèle comme exemple, et utilisons ces méthodes pour démontrer que ce modèle est capable d'oscillations induites par le retard. L'existence de telles oscillations est confirmée par simulation numérique. Nous découvrons de plus la possibilité d'oscillations complexes transitoires. Nous utilisons ensuite la structure de l'oscillophore identifié par nos méthodes, donc de la partie du réseau chimique responsable des oscillations, ainsi que notre connaissance de la longueur attendue d'un des retards, pour éliminer ce mécanisme hypothétique.

Mots-clés: instabilité induite par le retard, théorie des graphes, photosynthèse, photorespiration

1. Introduction

Graph theory plays an important role in various disciplines, ranging from computer science and engineering, to biology and sociology.[1] A thorough understanding of a complex system generally requires an integrative approach, i.e. a consideration of the system not as a simple assembly of elementary components, but as a connected whole. The connections can often usefully be thought to define a network represented by a graph.[2-17] The underlying machinery of cell biology and physiology consists of interconnected metabolic, genetic and signaling networks.[18-22] We can sometimes relate some particular behavior (e.g. multistability or oscillations) to properties of a suitable graphical representation of the network.[5,10,16,23-36] In particular, we recently developed a graphical analysis that provides a necessary condition for the generation of delay-induced instabilities in delayed mass-action systems.[33] Delayed terms have a number of uses in the modeling of biochemical systems.[37-48] Among other things, it has been shown that simple subnetworks (e.g. unbranched metabolic pathways) can often be replaced by delay elements while retaining the correct qualitative behavior of the model.[49,50]

Oscillations are often particularly revealing of regulatory interactions in biochemical systems.[51-55] Oscillations are common in many biological processes, for example, oscillations associated with the cell cycle,[56] circadian clock,[57] gene expression,[58] MAP kinase signaling,[59] etc. Oscillations in photosynthesis have been particularly intensively studied.[60-70] Recently, rapid, irregular oscillations of photosynthetic activity were observed upon transfer of a tobacco leaf to a low-CO_2 environment.[71] These oscillations are quite different in character from previously reported photosynthetic oscillations. We proposed a model for these oscillations in our

original report.[71] Roughly speaking, our hypothesis revolved around the competitive relationship between CO_2 and O_2 in the reactions catalyzed by the enzyme ribulose-1,5-bisphosphate carboxylase/oxygenase (Rubisco, EC 4.1.1.39). Under low-CO_2 conditions, oxygenation of ribulose-1,5-bisphosphate (RuBP) by Rubisco ought to become more important. Detoxification of one of the products of this reaction, 2-phosphoglycolate, eventually generates carbon dioxide in the mitochondria, which can diffuse back to the chloroplasts, tipping the balance toward the carboxylase function of Rubisco. Depletion of CO_2 by the carboxylase reaction then returns the system to its original low-CO_2 state, thus setting up conditions for oscillations.

Here, we analyze the model described above, showing that it is indeed capable of oscillations under certain conditions. The model includes two delays representing subnetworks with uncertain detailed kinetics. Each delay appears where an important product is generated after a sequence of steps which are not themselves of intrinsic interest.[49,72] The analysis is based on our graph-theoretical methods[32,33] and helps identify parameter ranges where oscillations are likely to be found. Guided by this analysis, we identify an oscillatory parameter range in numerical simulations. Our numerical explorations also uncovered a range in which transient chaos may be observed. Neither of these oscillatory regimes lies in a physiological range of parameters. This study highlights the power of graph-theoretical methods not only to identify the oscillatory potential of a chemical or biochemical network, but also to quickly determine if the oscillations lie in a plausible parameter range.

2. The model

The processes of photosynthesis and photorespiration are spread over several compartments. We built a compartmental model of these coupled processes that includes the substomatal space (the gas space inside a leaf), cytoplasm (the fluid that fills the main compartment of the cell), chloroplasts (the compartments containing the photosynthetic apparatus) and mitochondria (containing the respiratory machinery). The following subscripts were used to label compartments: atmospheric (atm), substomatal (ss), cytoplasmic (cyt), chloroplastic (chl), and mitochondrial (mito).

Figure 1 shows the key processes considered in our model, which takes the form of a set of coupled delay differential equations (DDEs). Atmospheric CO_2 and O_2 diffuse to and from the cytoplasmic space of leaf mesophyll tissue (the photosynthetic cells sandwiched between the epidermal cells of a leaf) through the substomatal space. Cytoplasmic CO_2 and O_2 diffuse into the chloroplast where they can respectively participate in the carboxylase and oxygenase reactions catalyzed by Rubisco.

The competitive kinetics of carboxylation and oxygenation of RuBP by Rubisco is central to our dynamical hypothesis regarding the observed oscillations.[71] We therefore treat this process in some detail. Rubisco has a complex activation biochemistry which involves the removal of inhibitory sugar phosphates and the activation of the enzyme by CO_2 and magnesium ions.[73] In the experiments modeled, leaves were kept in a normal CO_2 atmosphere in the light prior to their transfer to a low-CO_2 environment.[71] Recordings lasted only 10 minutes following the shift to low CO_2. Under these conditions, and considering the slow inactivation kinetics of Rubisco[74] relative to the time scale of the experiment, as well as the lack of an effect on the activation state of a

transfer to low CO_2,[75] the amount of activated Rubisco should be more or less constant, an assumption we make in this model, neglecting all forms of the enzyme other than the activated form. The enzyme Rubisco (E) reacts with RuBP to form the enzyme-substrate complex E^{RuBP}:

[1] $$E + RuBP \underset{k_{-6}}{\overset{k_6}{\rightleftharpoons}} E^{RuBP}$$

Once the complex E^{RuBP} has been formed it can either react with CO_2 or O_2, with probabilities depending on the ratio of CO_2 to O_2 in the chloroplast, as well as on the rate constants for these processes. The reaction of the complex E^{RuBP} with CO_2 produces the ternary complex $E_{CO_2}^{RuBP}$, which subsequently breaks down into two molecules of 3-phosphoglycerate (3PG), eventually resulting in the release of O_2 due to the light-dependent reactions of photosynthesis. To avoid including a detailed model of photosynthesis here, the eventual release of O_2 is represented as a delayed term, with delay τ_1.

[2] $$E^{RuBP} + CO_{2(chl)} \underset{k_{-7}}{\overset{k_7}{\rightleftharpoons}} E_{CO_2}^{RuBP}$$

[3] $$E_{CO_2}^{RuBP} \xrightarrow{k_8} E + O_{2(chl)}^{\tau_1}$$

The symbol $O_{2(chl)}^{\tau_1}$ represents O_2 formed in the chloroplast τ_1 time units after the breakdown of the $E_{CO_2}^{RuBP}$ complex due to the coupling between the Calvin cycle, of which Rubisco is the central enzyme, and the light-dependent reactions of photosynthesis. This coupling is not instantaneous as it requires several chemical and transport steps. Introducing a delay here is a convenient device to simplify our model[49,50,72] since we have no explicit interest here in the steps intervening between the carboxylation of RuBP by

Rubisco in reaction [3] and the synthesis of oxygen. Reaction [3] presents a cartoon of the coupling between the light-dependent and light-independent (Calvin-cycle) reactions of photosynthesis. This is sufficient since feedback via oxygen is almost certainly negligible at normal atmospheric concentrations of O_2. The production of oxygen by photosynthesis was introduced into the model because it has a small, but non-negligible, effect on the parameters at which oscillations are observed in numerical simulations. Photosynthetic oxygen production is however not essential to the generation of oxygen, and an early version of the model in which O_2 production was not considered was shown to oscillate (Md. R. Amin, unpublished).

Analogously, E^{RuBP} can react with O_2, making the complex $E_{O_2}^{RuBP}$, which goes on to form one molecule of 3PG and one molecule of 2-phosphoglycolate (2PG). The latter is toxic to plants and needs to be eliminated. The detoxification pathway for 2PG eventually leads to the production of serine and CO_2 in the mitochondria through a series of conversion steps involving several different compartments.[76] In the model, we represent this series of conversions as well at the necessary transport steps by introducing another delay τ_2. The modeled reaction chemistry for photorespiration is thus as follows:

[4] $$E^{RuBP} + O_{2(chl)} \underset{k_{-9}}{\overset{k_9}{\rightleftharpoons}} E_{O_2}^{RuBP}$$

[5] $$E_{O_2}^{RuBP} \xrightarrow{k_{10}} E + CO_{2(mito)}^{\tau_2}$$

where $CO_{2(mito)}^{\tau_2}$ represents carbon dioxide formed in the mitochondria τ_2 time units after the primary reaction event that produced an equivalent of 2PG.

As discussed above, over the time scale of the experiment, the concentration of active Rubisco ought to be roughly constant. Accordingly, we define the total amount of activated Rubisco by

$$[6] \qquad E_t = [\mathrm{E}] + [\mathrm{E}^{\mathrm{RuBP}}] + [\mathrm{E}^{\mathrm{RuBP}}_{\mathrm{CO}_2}] + [\mathrm{E}^{\mathrm{RuBP}}_{\mathrm{O}_2}]$$

Equation [6] will allow us to eliminate the concentration of the free activated enzyme, [E], in favor of the constant E_t and the concentrations of the complexes. The concentration of RuBP is also assumed constant since the hypothesis tested here is that the feedback between the action of Rubisco and photorespiratory carbon dioxide production is the oscillophore (the network motif generating oscillations[77]).

In compartmental modeling, mass conservation in transport processes is most naturally expressed by formulating the rates of transport across compartment boundaries in terms of fluxes given in units of number per unit time (e.g. mol s^{-1}).[78] The rate constants in Fig. 1 are flux rate constants, which might have units of L s^{-1} in the typical "chemical" system of units. Dividing one of these fluxes by the volume of a compartment thus gives the rate of change of concentration in the compartment due to the given flux. As an example, consider the net flux from the substomatal space (ss) to the cytoplasm (cyt):

$$[7] \qquad F_{\mathrm{CO}_2(\mathrm{ss}\to\mathrm{cyt})} = k_2\left[\mathrm{CO}_{2(\mathrm{ss})}\right] - k_{-2}\left[\mathrm{CO}_{2(\mathrm{cyt})}\right]$$

At equilibrium (zero flux), we have

$$[8] \qquad \frac{\left[\mathrm{CO}_{2(\mathrm{cyt})}\right]}{\left[\mathrm{CO}_{2(\mathrm{ss})}\right]} = \frac{k_2}{k_{-2}} = K_{\mathrm{CO}_2,\mathrm{cyt/ss}}$$

where $K_{CO_2,cyt/ss}$ is the cytoplasm to substomatal space partition coefficient. Using eq. [8], eq. [7] becomes

$$[9] \qquad F_{CO_2(ss\rightarrow cyt)} = k_2\left(\left[CO_{2(ss)}\right] - \left[CO_{2(cyt)}\right] / K_{CO_2,cyt/ss}\right)$$

The remaining fluxes are similarly given by the following equations:

$$[10] \qquad F_{CO_2(chl\rightarrow cyt)} = k_4\left(\left[CO_{2(chl)}\right] - \left[CO_{2(cyt)}\right] / K_{CO_2,cyt/chl}\right)$$

$$[11] \qquad F_{CO_2(mito\rightarrow cyt)} = k_5\left(\left[CO_{2(mito)}\right] - \left[CO_{2(cyt)}\right] / K_{CO_2,cyt/mito}\right)$$

$$[12] \qquad F_{O_2(ss\rightarrow cyt)} = k_1\left(\left[O_{2(ss)}\right] - \left[O_{2(cyt)}\right] / K_{O_2,cyt/ss}\right)$$

$$[13] \qquad F_{O_2(chl\rightarrow cyt)} = k_3\left(\left[O_{2(chl)}\right] - \left[O_{2(cyt)}\right] / K_{O_2,cyt/chl}\right)$$

We can now write down the delay-differential equations corresponding to the transport processes in Fig. 1 and reactions [1]–[5]. As usual, [X] represents the instantaneous concentration of the chemical species X, while $[X]_{t-\tau}$ represents the concentration of X at time $t-\tau$.

$$[14] \qquad \frac{d}{dt}\left[E^{RuBP}\right] = k_6\left[RuBP\right]\left(E_t - \left[E^{RuBP}\right] - \left[E^{RuBP}_{CO_2}\right] - \left[E^{RuBP}_{O_2}\right]\right) - k_{-6}\left[E^{RuBP}\right] - k_7\left[E^{RuBP}\right]\left[CO_{2(chl)}\right] + k_{-7}\left[E^{RuBP}_{CO_2}\right] + k_{-9}\left[E^{RuBP}_{O_2}\right] - k_9\left[E^{RuBP}\right]\left[O_{2(chl)}\right]$$

$$[15] \qquad \frac{d}{dt}\left[E^{RuBP}_{CO_2}\right] = k_7\left[E^{RuBP}\right]\left[CO_{2(chl)}\right] - k_{-7}\left[E^{RuBP}_{CO_2}\right] - k_8\left[E^{RuBP}_{CO_2}\right]$$

[16] $$\frac{d}{dt}\left[\mathrm{E}_{\mathrm{O}_2}^{\mathrm{RuBP}}\right] = k_9\left[\mathrm{E}^{\mathrm{RuBP}}\right]\left[\mathrm{O}_{2(\mathrm{chl})}\right] - k_{-9}\left[\mathrm{E}_{\mathrm{O}_2}^{\mathrm{RuBP}}\right] - k_{10}\left[\mathrm{E}_{\mathrm{O}_2}^{\mathrm{RuBP}}\right]$$

[17] $$\frac{d}{dt}\left[\mathrm{CO}_{2(\mathrm{cyt})}\right] = \left(F_{\mathrm{CO}_2(\mathrm{mito}\to\mathrm{cyt})} + F_{\mathrm{CO}_2(\mathrm{ss}\to\mathrm{cyt})} + F_{\mathrm{CO}_2(\mathrm{chl}\to\mathrm{cyt})}\right)/V_{\mathrm{cyt}}$$

[18] $$\frac{d}{dt}\left[\mathrm{CO}_{2(\mathrm{ss})}\right] = \phi_{\mathrm{CO}_2}\left(\left[\mathrm{CO}_{2(\mathrm{atm})}\right] - \left[\mathrm{CO}_{2(\mathrm{ss})}\right]\right) - F_{\mathrm{CO}_2(\mathrm{ss}\to\mathrm{cyt})}/V_{\mathrm{ss}}$$

[19] $$\frac{d}{dt}\left[\mathrm{CO}_{2(\mathrm{mito})}\right] = k_{10}\left[\mathrm{E}_{\mathrm{O}_2}^{\mathrm{RuBP}}\right]_{t-\tau_2} - F_{\mathrm{CO}_2(\mathrm{mito}\to\mathrm{cyt})}/V_{\mathrm{mito}}$$

[20] $$\frac{d}{dt}\left[\mathrm{CO}_{2(\mathrm{chl})}\right] = k_{-7}\left[\mathrm{E}_{\mathrm{CO}_2}^{\mathrm{RuBP}}\right] - k_7\left[\mathrm{E}^{\mathrm{RuBP}}\right]\left[\mathrm{CO}_{2(\mathrm{chl})}\right] - F_{\mathrm{CO}_2(\mathrm{chl}\to\mathrm{cyt})}/V_{\mathrm{chl}}$$

[21] $$\frac{d}{dt}\left[\mathrm{O}_{2(\mathrm{cyt})}\right] = \left(F_{\mathrm{O}_2(\mathrm{ss}\to\mathrm{cyt})} + F_{\mathrm{O}_2(\mathrm{chl}\to\mathrm{cyt})}\right)/V_{\mathrm{cyt}}$$

[22] $$\frac{d}{dt}\left[\mathrm{O}_{2(\mathrm{ss})}\right] = \phi_{\mathrm{O}_2}\left(\left[\mathrm{O}_{2(\mathrm{atm})}\right] - \left[\mathrm{O}_{2(\mathrm{ss})}\right]\right) - F_{\mathrm{O}_2(\mathrm{ss}\to\mathrm{cyt})}/V_{\mathrm{ss}}$$

[23] $$\frac{d}{dt}\left[\mathrm{O}_{2(\mathrm{chl})}\right] = k_{-9}\left[\mathrm{E}_{\mathrm{O}_2}^{\mathrm{RuBP}}\right] - k_9\left[\mathrm{E}^{\mathrm{RuBP}}\right]\left[\mathrm{O}_{2(\mathrm{chl})}\right] + k_8\left[\mathrm{E}_{\mathrm{CO}_2}^{\mathrm{RuBP}}\right]_{t-\tau_1} - F_{\mathrm{O}_2(\mathrm{chl}\to\mathrm{cyt})}/V_{\mathrm{chl}}$$

Note the delayed terms in eqs. [19] and [23].The full model consists of eqs. [9]–[13] and [14]–[23].

3. Graph-theoretical analysis of the model

The experiments displayed rapid oscillations in the photosynthetic observables.[71] We thus set out to determine if the model described above was capable of oscillations. Estimates of every single parameter in the model were obtained, as reported elsewhere.[79] Of course, many estimates of biochemical parameters are subject to significant uncertainty. When the model failed to display oscillations following a manual, and

necessarily incomplete, search of the plausible parameter space, we turned to a graph-theoretical analysis to determine whether it was at all possible for this model to oscillate, and to provide some guidance regarding relevant parameter regimes. As shown below, the analysis revealed that the model can oscillate only when τ_2, the delay associated with the photorespiratory synthesis of CO_2, is nonzero.

The analysis of both the zero-delay (ordinary differential equation, ODE) and delayed versions of the model requires the construction of the same bipartite graph for the reaction[32,33] (Fig. 2). Bipartite graphs have two distinct types of vertices, in this case chemical species (circled) and reaction (boxed) vertices. Arrows, known as **arcs** in this theory, point from reactant vertices to reaction vertices, and from reaction vertices to product vertices. Thus, there is a simple one-to-one relationship between the reaction mechanism as normally written and the bipartite graph. (Stoichiometric coefficients that differ from unity appear in the graph as weights of the corresponding edges, allowing for the representation of mechanisms with arbitrary stoichiometry.) Except for gas exchange with the atmosphere (where a reasonably obvious convention was adopted), the reactions in Fig. 2 are numbered as in Fig. 1 and reactions [1]–[5]. Bold arcs denote delayed product formation.

We now define several terms required for the analysis.[32] Note that some of the definitions used here and in our previous work have more restricted meanings than in conventional graph theory. An **edge**, denoted [X,R], is an arc from a reactant (X) to a reaction (R) vertex. An example of an edge from Fig. 2 is [RuBP,R_6]. A **positive path**, denoted [X,R,Y], is a reactant-product relationship between the reactant X and product Y through the reaction R, such as [RuBP,R_6,E^{RuBP}]. A **negative path**, $[\overline{X,R,Y}]$, corresponds

to X and Y both being reactants in reaction R. In Fig. 2, $\overline{[\mathrm{RuBP},\mathrm{R}_6,\mathrm{E}]}$ is a negative path as is, of course, $\overline{[\mathrm{E},\mathrm{R}_6,\mathrm{RuBP}]}$. Note that paths and edges always start from a reactant, never from a product. A **cycle** is a sequence of distinct paths in which the last vertex of one path is the first vertex of the next, and the last vertex of the last path included is the first vertex of the first path. A cycle is **positive** if it contains an even number of negative paths and **negative** if it contains an odd number of negative paths. A **subgraph** is a set of edges and/or cycles such that each chemical species vertex in the subgraph is the beginning of only one edge or path. This makes the edges and cycles included in the subgraph mutually disjoint. The **order** of a subgraph is the number of chemical species vertices included in the subgraph. A **fragment** of order *k* is the union of all subgraphs of order *k* that can be built from the same set of chemical species and reaction vertices.

Figure 3 shows one particular fragment of order 6 (which will be key to our analysis of this mechanism and denoted S_6) and its subgraphs (g_1 to g_3). Each subgraph consists of disjoint edges and cycles: g_1 is the edge subgraph, which we always find among the subgraphs of a fragment; g_2 consists of a positive cycle (no negative paths) and a set of edges; and g_3 consists of a large negative cycle (due to the single negative path $\overline{[\mathrm{CO}_{2(\mathrm{chl})},\mathrm{R}_7,\mathrm{E}^{\mathrm{RuBP}}]}$) and one edge. As an exercise in cycle construction, let us consider the large cycle in g_3. Starting from any one of the chemical species vertices, follow the cycle in a clockwise direction, noting that it is composed entirely of paths, all of which are positive except for the one negative path identified above. It is not possible to traverse the cycle in a counterclockwise direction since it is impossible to get all the way around by following proper paths, which must always start at a reactant, i.e. follow the direction of an arc from a chemical species to a reaction vertex. The second part of a

path on the other hand, from the reaction vertex to a chemical species, can go against the arrow of an arc, and indeed does in a negative path. No other subgraphs can be constructed from this fragment following the rules outlined above.

It turns out that each fragment corresponds to a term in the characteristic equation arising in the stability analysis of a chemical reaction mechanism.[25,32,80] Critical fragments (defined below) will correspond to negative terms in the characteristic equation, which are necessary to obtain instabilities leading to oscillations.

Let α_{RX} be the stoichiometric coefficient of the reactant X in reaction R, and β_{RY} be the stoichiometric coefficient of product Y in reaction R. For a cycle *C*, we define

$$K_C = \prod_{[X,R,Y]\in C} \alpha_{RX}\beta_{RY} \prod_{[X,R,Y]\in C} \left(-\alpha_{RX}\alpha_{RY}\right) \qquad [24]$$

Note that each negative path contributes a factor of -1 to the product. Thus, a positive cycle has a positive value of K_C, and a negative cycle has a negative value of K_C. A subgraph *g* is associated with a coefficient

$$K_g = \left(-1\right)^{\chi_g} \prod_{C\in g} K_C \prod_{[X,R]\in g} \alpha_{RX}^2 \qquad [25]$$

where χ_g is the number of cycles in *g*. Finally, we can compute the **criticality index** of a fragment of order *k*, S_k, by

$$K_{S_k} = \sum_{g\in S_k} K_g \qquad [26]$$

If $K_{S_k} < 0$, then S_k is a **critical fragment**. The existence of a critical fragment is a necessary condition for a Hopf bifurcation leading to oscillatory solutions.[10,25,81] From eq. [26], we see that there must be at least one subgraph with a negative K_g to get a negative value of K_{S_k}. Equation [25] in turn implies that to get a negative K_g, there must

be an odd number of positive cycles in a subgraph. To see this, write $\chi_g = \chi_+ + \chi_-$, where χ_+ is the number of positive cycles in a subgraph, and χ_- is the number of negative cycles. Thus,

[27] $$(-1)^{\chi_g} = (-1)^{\chi_+}(-1)^{\chi_-}$$

In eq. [25], χ_- of the K_C values are negative. The sign of $(-1)^{\chi_-}$ therefore cancels with the signs of the χ_- negative K_C values. The sign of K_g is therefore $(-1)^{\chi_+}$, which is negative only if χ_+ is odd.

A careful search through the mechanism found no critical fragments associated with the ODE (zero-delay) model,[79] precluding oscillations in the absence of delays. We confirmed the nonexistence of a critical fragment in the undelayed case using GraTeLPy, a new software package that automates this task for the ODE case.[82] There remains the possibility of delay-induced oscillations, i.e. of oscillations that are only possible because of the delays in the model.[83] The analysis of the delay model is similar to that of the ODE model, except that K_C (eq. [24]) is replaced by[33]

[28] $$\hat{K}_C = \prod_{[X,R,Y]\in C} \alpha_{RX}\beta_{RY} \prod_{[X,R,Y]\in C} \alpha_{RX}\alpha_{RY}$$

(We use a circumflex to denote any quantity associated with the delay model.) A delay-induced instability is only possible if, additionally, the critical fragment includes a delayed product-formation arc. Given that $\hat{K}_C$ must be positive, $\hat{K}_{S_k}$ (calculated analogously to K_{S_k}) can now only be negative due to the factor of $(-1)^{\chi_g}$ in eq. [25] (or, more precisely, the analog of eq. [25] calculated using $\hat{K}_C$). Hopf bifurcations are thus possible if at least one of the subgraphs of a fragment has an odd number of cycles. If

there is an odd number of positive cycles, then this instability already arises in the ODE system and cannot be said to be delay-induced. Accordingly, a delay-induced instability requires an odd number of negative cycles among an odd number of cycles, the so-called **odd-odd condition**.[33]

In the model studied here, there is a critical fragment of order six, namely

$$[29] \quad S_6 = \begin{pmatrix} E^{RuBP} & E^{RuBP}_{O_2} & CO_{2(mito)} & CO_{2(cyt)} & CO_{2(chl)} & E^{RuBP}_{CO_2} \\ R_9 & R_{10} & R_5 & R_{-4} & R_7 & R_{-7} \end{pmatrix}$$

The critical fragment is specified above by its chemical species (first row) and reaction (second row) vertex sets. This critical fragment appears in Fig. 2 as dotted arcs, and is extracted for clearer viewing in Fig. 3 along with its subgraphs. The large cycle in S_6 is, as noted above, a negative cycle. This cycle appears in the subgraph g_3, which contains no other cycles, so that this subgraph satisfies the odd-odd condition. Moreover, the fragment includes the delayed formation of CO_2 in the mitochondria by reaction R_{10}. This is important because delay-induced instabilities can only arise due to fragments that actually contain a delay. To show that the fragment is indeed critical, we need to calculate $\hat{K}_{S_6}$. First note that in this model, all the stoichiometric coefficients are unity, so from eqs. [25] and [28], $\hat{K}_g$ simplifies to $(-1)^{\chi_g}$. The edge subgraph g_1 has no cycles ($\chi_g = 0$) so $\hat{K}_{g_1} = 1$. Both g_2 and g_3 have $\chi_g = 1$, so $\hat{K}_{g_2} = \hat{K}_{g_3} = -1$. Accordingly, $\hat{K}_{S_6} = \hat{K}_{g_1} + \hat{K}_{g_2} + \hat{K}_{g_3} = -1$, and thus S_6 is a critical fragment of the delay model.

As an aside, for the ODE model, the calculation is much the same except that, according to eq. [24], the negative cycle in g_3 is associated with a negative value of K_C

whose sign then cancels the sign of the $(-1)^{\chi_g}$ in the calculation of K_{g_3}. Consequently, K_{S_6} works out to +1 instead of -1, so S_6 is not critical in the model without delays.

No other critical fragments of order six or lower can be found in the bipartite graph of the DDE model.[79] We were unable to find critical fragments of order greater than six, although the bipartite graph is sufficiently complex that we cannot guarantee that such fragments do not exist, and critical fragments of order up to nine (given that there are ten variables in the model) may be relevant.[32,33] At present, there is no software available to identify critical fragments of delay models, although it should be straightforward to modify GraTeLPy[82] to do so.

4. Numerical simulations

We mentioned at the beginning of the last section that an initial numerical exploration failed to uncover oscillations. In such cases, it is difficult to tell whether the problem is the inability of the model to generate oscillations, or our inability to locate appropriate parameter values. The analysis of section 3 showed that the model could quite likely generate oscillations. (This is not a certitude because the existence of a critical fragment is only a necessary, not a sufficient condition for oscillations.[33] However, our experience has been that it is generally possible to find parameters yielding oscillations if the bipartite graph has a critical fragment.) This analysis also suggests the parameter values most worth exploring in detail, namely those involved in the critical fragment. The other parameter values may become important to adjust steady-state levels of species in the critical fragment, but the need for such adjustments are typically fairly

obvious (e.g. if the steady-state concentration of a species in the critical fragment is either extraordinarily low or extraordinarily high). The identification of the critical fragment led to the rapid discovery of oscillations by adjusting the initial set of rate constants estimated from the literature using the graph-theoretical analysis for guidance.

Figure 4 shows transient irregular oscillations obtained for one particular set of parameters. The model equations were integrated using the dynamical systems software XPPAUT (version 6.11).[84] These irregular transients eventually give way to limit-cycle oscillations (Fig. 5). Unfortunately, the parameters at which these oscillations were obtained are not physiologically plausible, with some parameters deviating by a few orders of magnitude from our best estimates,[79] and the oscillations have much too long a period compared to those observed experimentally.[71] We have found oscillations in other parameter regimes (based on the same critical fragment, but with a different balance between one reaction and another), but in no case have we been able to generate rapid oscillations with fully physiologically plausible parameters.[79] These results suggest rather strongly that we either have the wrong mechanism altogether for these oscillations, or that some important biochemical interaction is missing.

5. Discussion and conclusion

The model analyzed in this article is not particularly large by the standards of modern systems biology, with 10 variables (concentrations) and 30 parameters. Still, convincing oneself that the ODE model cannot generate oscillations using conventional methods of bifurcation theory would likely be all but impossible, and determining that the delay model does have oscillatory solutions would likewise challenge the best analysts.

As shown by our early, unsuccessful numerical explorations, an unaided search of a high-dimensional parameter space is also difficult. The graph-theoretical analysis deployed here enables us to locate, by visual inspection, the presence or absence of structures within the reaction network that may lead to oscillatory behavior. All possible critical fragments with up to four interacting chemical species have been enumerated for the ODE case.[26,81] Until recently, the task of finding high-order critical fragments was a difficult one, although not impossible as shown by our discovery, by visual inspection and hand calculation, of a critical fragment of 6th order in the DDE model.[79] Software has just become available to automate this task for the ODE case.[82] As noted earlier, it should be straightforward to adapt this software to the calculation of critical fragments of delay models.

We can generalize our conclusions somewhat. One possible objection to our model is that the stoichiometry of photorespiration is not one carbon dioxide for every RuBP oxygenated, but is somewhat lower since there are alternative metabolic fates available to the intermediate products of the 2-phosphoglycolate detoxification pathway.[85] The edge corresponding to the delayed formation of CO_2 in the mitochondria only appears in subgraph g_3. Let the stoichiometric coefficient for the delayed formation of $CO_{2(mito)}$ be $\beta < 1$, keeping all other aspects of the model unchanged. For the large cycle in g_3, $\hat{K}_C = \beta$ by eq. [28]. Thus, $\hat{K}_{g_3} = -\beta$ (by eq. [25]), so that $\hat{K}_{S_6} = -\beta$ since the contributions of g_1 and g_2 still cancel out. Accordingly, the fragment identified in Fig. 3 is critical regardless of the stoichiometry of photorespiration, and we would therefore expect to be able to find parameters leading to oscillations even if $\beta < 1$. This parameter range would likely become narrower as β decreases, and must vanish at $\beta = 0$. Using

graph-theoretical methods of analysis of reaction networks, we come to these conclusions with relatively little effort.

Another possible criticism of our model is the absence of mitochondrial respiration. This is relatively insignificant in the light at low CO_2.[86] Including a reasonable value for the flux through the respiratory pathway has very little effect on the behavior of the model (K. Wynnyk, unpublished).

It might also be argued that the suppressed biochemistry, which was replaced by the delays τ_1 and τ_2, involves nonlinearities whose detailed modeling might alter the conclusions of this study. Past experience suggests that there are no significant dynamical differences when subsystems with simple kinetics (including Michaelis-Menten kinetics) are eliminated via the introduction of a delay.[49,50] Nontrivial feedback might of course change the situation. In this study, we have shown that delayed recycle of CO_2, which is included in the critical fragment, is, in and of itself, sufficient to permit oscillatory behavior. Stronger nonlinearities in the recycle loop might facilitate oscillations, but are not necessary.

Restating our central result, we were able to show that a proposal for the genesis of rapid oscillations in leaves transferred to a low-CO_2 atmosphere[71] can generate oscillatory solutions, but that these solutions are only obtained at unrealistic parameter values and that, moreover, these oscillations have periods that are inconsistent with experiment. Accordingly, we can state with some certainty that the hypothesis enunciated in our earlier paper is either wrong or, at best, that our model lacks a critical biochemical interaction. Regarding the period of oscillations, the trouble, in a nutshell, is the very long delay arising between the oxygenation of RuBP and the appearance of photorespiratory

CO_2 in the mitochondria (τ_2, estimated to be of the order of several tens of seconds[87]). Given that the critical fragment includes the term delayed by τ_2 and that this delayed feedback is necessary to induce oscillations, the period must be of the same order of magnitude as this delay. For the oscillations shown in Fig. 5, τ_2 = 40 s, and the period is 28.65 s. Oscillations with a period of a few seconds cannot be recovered if the oscillophore is the fragment shown in Fig. 3. The oscillations observed in the experiment must therefore be due to a critical fragment with a different delayed loop with a much smaller delay. It is tempting to look for a critical fragment involving the much shorter delay τ_1. However, our current model does not include a critical fragment involving τ_1, again leading to the conclusion that some biochemistry is missing. One possibility for the missing pathway might be the coupling between RuBP recycling and the Calvin cycle. It is highly unlikely that RuBP could remain constant during these oscillations, as assumed in our model, and it is possible that the interplay between RuBP recycling and the reactions catalyzed by Rubisco would account for the observed oscillations.

This contribution illustrates the use of graph-theoretical methods to solve problems in chemical or biochemical modeling. The ability to rule out candidate mechanisms is just as important in biochemical modeling as the validation of plausible mechanisms. In this case, we have shown that a particular hypothesis for oscillations observed after transferring leaves to a low-CO_2 atmosphere is either incorrect or, at best, incomplete. Candidate mechanisms can be ruled out at one of two stages based on the methods proposed here. A mechanism for an oscillatory system must have an oscillophore or, in the language of bipartite graph analysis, a critical fragment. Our model passed this first test, provided we included the delay inherent in the photorespiratory

pathway. Although numerical simulations subsequently showed oscillations, the structure of the oscillophore and in particular the presence of a long delay within this oscillophore subsequently ruled out the proposed mechanism. In other words, the identification of the oscillophore helped us to focus our attention on a manageable subset of the biochemistry, leading to insights that would have been difficult to obtain from Fig. 1 and numerical simulations alone.

Acknowledgements

The authors would like to thank Dr Maya Mincheva of Northern Illinois University for bringing the software GraTeLPy developed by her and her colleagues to our attention, and Georg Walther of the Department of Computational and Systems Biology at the John Innes Centre for his help in interpreting the output. This work was supported by the Natural Sciences and Engineering Research Council of Canada.

References

(1) Pavlopoulos, G. A.; Secrier, M.; Moschopoulos, C. N.; Soldatos, T. G.; Kossida, S.; Aerts, J.; Schneider, R.; Bagos, P. G. *BioData Mining* **2011**, *4*, 10.

(2) Christiansen, J. A. *Adv. Catal.* **1953**, *5*, 311.

(3) Mason, S. J. *Proc. Inst. Radio Eng.* **1953**, *41*, 1144.

(4) King, E. L.; Altman, C. *J. Phys. Chem.* **1956**, *60*, 1375.

(5) Beretta, E.; Vetrano, F.; Solimano, F.; Lazzari, C. *Bull. Math. Biol.* **1979**, *41*, 641.

(6) Galvez, J.; Varon, R. *J. Theor. Biol.* **1981**, *89*, 1.

(7) Sinanoğlu, O. *J. Math. Phys.* **1981**, *22*, 1504.

(8) Goldstein, B. N.; Shevelev, E. L. *J. Theor. Biol.* **1985**, *112*, 493.

(9) Feinberg, M. *Chem. Eng. Sci.* **1987**, *42*, 2229.

(10) Goldstein, B. N.; Ivanova, A. N. *FEBS Lett.* **1987**, *217*, 212.

(11) Reder, C. *Biomed. Biochim. Acta* **1990**, *49*, 671.

(12) Zeigarnik, A. V.; Temkin, O. N. *Kinet. Catal.* **1994**, *35*, 647.

(13) Grossman, J. W.; Ion, P. D. F. *Congr. Numer.* **1995**, *108*, 129.

(14) Balinski, M.; Ratier, G. *SIAM Rev.* **1997**, *39*, 575.

(15) Holme, P.; Huss, M.; Jeong, H. *Bioinformatics* **2003**, *19*, 532.

(16) Gatermann, K.; Eiswirth, M.; Sensse, A. *J. Symbolic Comput.* **2005**, *40*, 1361.

(17) Spivak, S. I.; Ismagilova, A. S.; Khamitova, I. A. *Dokl. Phys. Chem.* **2010**, *434*, 169.

(18) Hartwell, L. H.; Hopfield, J. J.; Leibler, S.; Murray, A. W. *Nature* **1999**, *402*, C47.

(19) Kohn, K. W. *Chaos* **2001**, *11*, 84.

(20) Newman, M. E. J. *SIAM Rev.* **2003**, *45*, 167.

(21) Wilkins, A. S. *BioEssays* **2007**, *29*, 1179.

(22) Kestler, H. A.; Wawra, C.; Kracher, B.; Kühl, M. *BioEssays* **2008**, *30*, 1110.

(23) Goldstein, B. N.; Selivanov, V. A. *Biomed. Biochim. Acta* **1990**, *49*, 645.

(24) Schlosser, P. M.; Feinberg, M. *Chem. Eng. Sci.* **1994**, *49*, 1749.

(25) Ermakov, G. L. *Biochemistry (Moscow)* **2003**, *68*, 1109.

(26) Ermakov, G. L. *Biochemistry (Moscow)* **2003**, *68*, 1121.

(27) Goldstein, B. N.; Ermakov, G.; Centelles, J. J.; Westerhoff, H. V.; Cascante, M. *Eur. J. Biochem.* **2004**, *271*, 3877.

(28) Craciun, G.; Feinberg, M. *SIAM J. Appl. Math.* **2005**, *65*, 1526.

(29) Craciun, G.; Feinberg, M. *SIAM J. Appl. Math.* **2006**, *66*, 1321.

(30) Craciun, G.; Feinberg, M. *IEE Proc. Syst. Biol.* **2006**, *153*, 179.

(31) Mincheva, M.; Roussel, M. R. *J. Chem. Phys.* **2006**, *125*, 204102.

(32) Mincheva, M.; Roussel, M. R. *J. Math. Biol.* **2007**, *55*, 61.

(33) Mincheva, M.; Roussel, M. R. *J. Math. Biol.* **2007**, *55*, 87.

(34) Shinar, G.; Feinberg, M. *Science* **2010**, *327*, 1389.

(35) Mincheva, M. *Bull. Math. Biol.* **2011**, *73*, 2277.

(36) Mincheva, M.; Roussel, M. R. *Math. Biosci.* **2012**, *240*, 1.

(37) MacDonald, N. *J. Theor. Biol.* **1977**, *67*, 549.

(38) Painter, P. R.; Bliss, R. D. *J. Theor. Biol.* **1981**, *90*, 293.

(39) Mahaffy, J. M. *J. Theor. Biol.* **1984**, *106*, 89.

(40) Laisk, A.; Walker, D. A. *Proc. R. Soc. London, Ser. B* **1986**, *227*, 281.

(41) Smolen, P.; Baxter, D. A.; Byrne, J. H. *Am. J. Physiol.* **1998**, *274*, C531.

(42) Drew, D. A. *Bull. Math. Biol.* **2001**, *63*, 329.

(43) Lewis, J. *Curr. Biol.* **2003**, *13*, 1398.

(44) Monk, N. A. M. *Curr. Biol.* **2003**, *13*, 1409.

(45) Bratsun, D.; Volfson, D.; Tsimring, L. S.; Hasty, J. *Proc. Natl. Acad. Sci. U.S.A.* **2005**, *102*, 14593.

(46) Wang, R.; Jing, Z.; Chen, L. *Bull. Math. Biol.* **2005**, *67*, 339.

(47) Barrio, M.; Burrage, K.; Leier, A.; Tian, T. *PLoS Comput. Biol.* **2006**, *2*, e117.

(48) Srividhya, J.; Gopinathan, M. S.; Schnell, S. *Biophys. Chem.* **2007**, *125*, 286.

(49) Roussel, C. J.; Roussel, M. R. *Phys. Can.* **2001**, *57*, 114.

(50) Hinch, R.; Schnell, S. *J. Math. Chem.* **2004**, *35*, 253.

(51) Nguen, T. T. F.; Karelina, T. A.; Kukushkin, A. K. *Biophysics* **2007**, *52*, 468.

(52) Aon, M. A.; Cortassa, S.; Westerhoff, H. V.; Berden, J. A.; van Spronsen, E.; Van Dam, K. *J. Cell Sci.* **1991**, *99*, 325.

(53) Karavayev, V. A.; Kukushkin, A. K. *Biophysics* **1993**, *38*, 987.

(54) Murray, D. B.; Engelen, F.; Lloyd, D.; Kuriyama, H. *Microbiology* **1999**, *145*, 2739.

(55) Sohn, H.-Y.; Kuriyama, H. *Arch. Microbiol.* **2001**, *176*, 69.

(56) Tyson, J. J. *Proc. Natl. Acad. Sci. U.S.A.* **1991**, *88*, 7328.

(57) Goldbeter, A. *Proc. R. Soc. London, Ser. B* **1995**, *261*, 319.

(58) Goodwin, B. C. *Advan. Enzyme Regul.* **1965**, *3*, 425.

(59) Chickarmane, V.; Kholodenko, B. N.; Sauro, H. M. *J. Theor. Biol.* **2007**, *244*, 68.

(60) van der Veen, R. *Physiol. Plant.* **1949**, *2*, 287.

(61) Wilson, A. T.; Calvin, M. *J. Am. Chem. Soc.* **1955**, *77*, 5948.

(62) Ogawa, T. *Biochim. Biophys. Acta* **1982**, *681*, 103.

(63) Walker, D. A.; Sivak, M. N.; Prinsley, R. T.; Cheesbrough, J. K. *Plant Physiol.* **1983**, *73*, 542.

(64) Furbank, R. T.; Foyer, C. H. *Arch. Biochem. Biophys.* **1986**, *246*, 240.

(65) Sharkey, T. D.; Stitt, M.; Heineke, D.; Gerhardt, R.; Raschke, K.; Heldt, H. W. *Plant Physiol.* **1986**, *81*, 1123.

(66) Stitt, M.; Grosse, H.; Woo, K.-C. *J. Plant Physiol.* **1988**, *133*, 138.

(67) Laisk, A.; Siebke, K.; Gerst, U.; Eichelmann, H.; Oja, V.; Heber, U. *Planta* **1991**, *185*, 554.

(68) Siebke, K.; Weis, E. *Photosynth. Res.* **1995**, *45*, 225.

(69) Ferimazova, N.; Küpper, H.; Nedbal, L.; Trtílek, M. *Photochem. Photobiol.* **2002**, *76*, 501.

(70) Lazár, D.; Kaňa, R.; Klinkovský, T.; Nauš, J. *Photosynthetica* **2005**, *43*, 13.

(71) Roussel, M. R.; Ivlev, A. A.; Igamberdiev, A. U. *J. Plant Physiol.* **2007**, *164*, 1188.

(72) Roussel, M. R. *J. Phys. Chem.* **1996**, *100*, 8323.

(73) Spreitzer, R. J.; Salvucci, M. E. *Annu. Rev. Plant Biol.* **2002**, *53*, 449.

(74) von Caemmerer, S.; Quick, W. P. In *Photosynthesis: Physiology and Metabolism*; Leegood, R. C., Sharkey, T. D., von Caemmerer, S., Eds.; Kluwer: Dordrecht, 2000, p 85.

(75) Martindale, W.; Bowes, G. *J. Exp. Bot.* **1996**, *47*, 781.

(76) Nelson, D. L.; Cox, M. M. *Lehninger Principles of Biochemistry*; 4th ed.; Freeman: New York, 2005.

(77) Boiteux, A.; Hess, B. *Faraday Symp. Chem. Soc.* **1974**, *9*, 202.

(78) Rubinow, S. I. *Bull. Am. Math. Soc.* **1975**, *81*, 782.

(79) Amin, M. R. Master's thesis, University of Lethbridge, 2012, https://www.uleth.ca/dspace/handle/10133/3260.

(80) Ivanova, A. N.; Tarnopol'skii, B. L. *Kinet. Catal.* **1979**, *20*, 1271.

(81) Ermakov, G. L.; Goldstein, B. N. *Biochemistry (Moscow)* **2002**, *67*, 473.

(82) Walther, G. R.; Hartley, M.; Mincheva, M. GraTeLPy 0.1.0; 2013; https://pypi.python.org/pypi/GraTeLPy.

(83) Bélair, J.; Campbell, S. A.; van den Driessche, P. *SIAM J. Appl. Math.* **1996**, *56*, 245.

(84) Ermentrout, B. *Simulating, Analyzing, and Animating Dynamical Systems*; SIAM: Philadelphia, 2002.

(85) Hanson, K. R.; Peterson, R. B. *Arch. Biochem. Biophys.* **1987**, *252*, 591.

(86) Laisk, A.; Sumberg, A. *Plant Physiol.* **1994**, *106*, 689.

(87) Atkin, O. K.; Millar, A. H.; Gardeström, P.; Day, D. A. In *Photosynthesis: Physiology and Metabolism*; Leegood, R. C., Sharkey, T. D., von Caemmerer, S., Eds.; Kluwer: Dordrecht, 2000, p 153.

Figure captions

Fig. 1. Diagram of the model showing transport between the compartments and key reaction processes. The following subscripts are used to denote compartments: atmospheric (atm), substomatal (ss), cytoplasmic (cyt), chloroplastic (chl), and mitochondrial (mito). $O_{2(chl)}^{\tau_1}$ denotes molecular oxygen produced in the chloroplasts by photosynthesis τ_1 time units following the carboxylation of RuBP, while $CO_{2(mito)}^{\tau_2}$ denotes CO_2 appearing in the mitochondria τ_2 time units following the oxygenation of RuBP.

Fig. 2. The bipartite graph corresponding to the reactions and transport of CO_2 and O_2 through the plant leaf. Circles represent chemical species while boxes represent reactions. The numbering of the reactions is as in Fig. 1 and reactions [1]–[5], except that exchange with the atmosphere required slightly different symbols. Delayed product formation is represented by bold arcs. Dotted arcs represent the small cycle and dashed arcs represent the large cycle in the critical fragment. (The two cycles share the $CO_{2(chl)} \rightarrow R_7$ arc.)

Fig. 3. The critical fragment S_6 along with its subgraphs g_1, g_2 and g_3.

Fig. 4. Irregular transient oscillations obtained at the following parameter values: $k_1 = k_2 = 10^{-2}$ L s^{-1}, $k_3 = 1$ L s^{-1}, $k_4 = 1.5\times10^{-3}$ L s^{-1}, $k_5 = 0.15$ L s^{-1}, $k_6 = 10^5$ mM^{-1} s^{-1}, $k_{-6} = 270$ s^{-1}, $k_7 = 60$ mM^{-1} s^{-1}, $k_{-7} = 10^{-7}$ s^{-1}, $k_8 = 3\times10^{-3}$ s^{-1}, $k_9 = 250$ mM^{-1} s^{-1}, $k_{-9} = k_{10} = 120$ s^{-1}, $\phi_{CO_2} = 1.84$ s^{-1}, $\phi_{O_2} = 0.0453$ s^{-1}, $\tau_1 = 1$ s, $\tau_2 = 40$ s, $[O_{2(atm)}] = 8.73$ mM, $[CO_{2(atm)}] = 1.5\times10^{-3}$ mM, [RuBP] = 1.6 mM, $E_t = 4$ mM, $K_{CO_2,cyt/chl} = 0.1$, $K_{CO_2,cyt/ss} = 1$,

$K_{CO_2,cyt/mito} = 0.5$, $K_{O_2,cyt/chl} = K_{O_2,cyt/ss} = 10$, V_{chl} = 890 μL, V_{mito} = 28 μL, V_{cyt} = 186 μL and V_{ss} = 1600 μL. All initial conditions were set to zero, including the initial functions required for the delay terms. Panel (b) shows the same trajectory segment as panel (a) plotted as a projection onto the ($[CO_{2(chl)}]$,$[O_{2(chl)}]$) plane.

Fig. 5. Limit cycle obtained after the decay of the transient shown in Fig. 4. The period of the oscillations is 28.65 s.

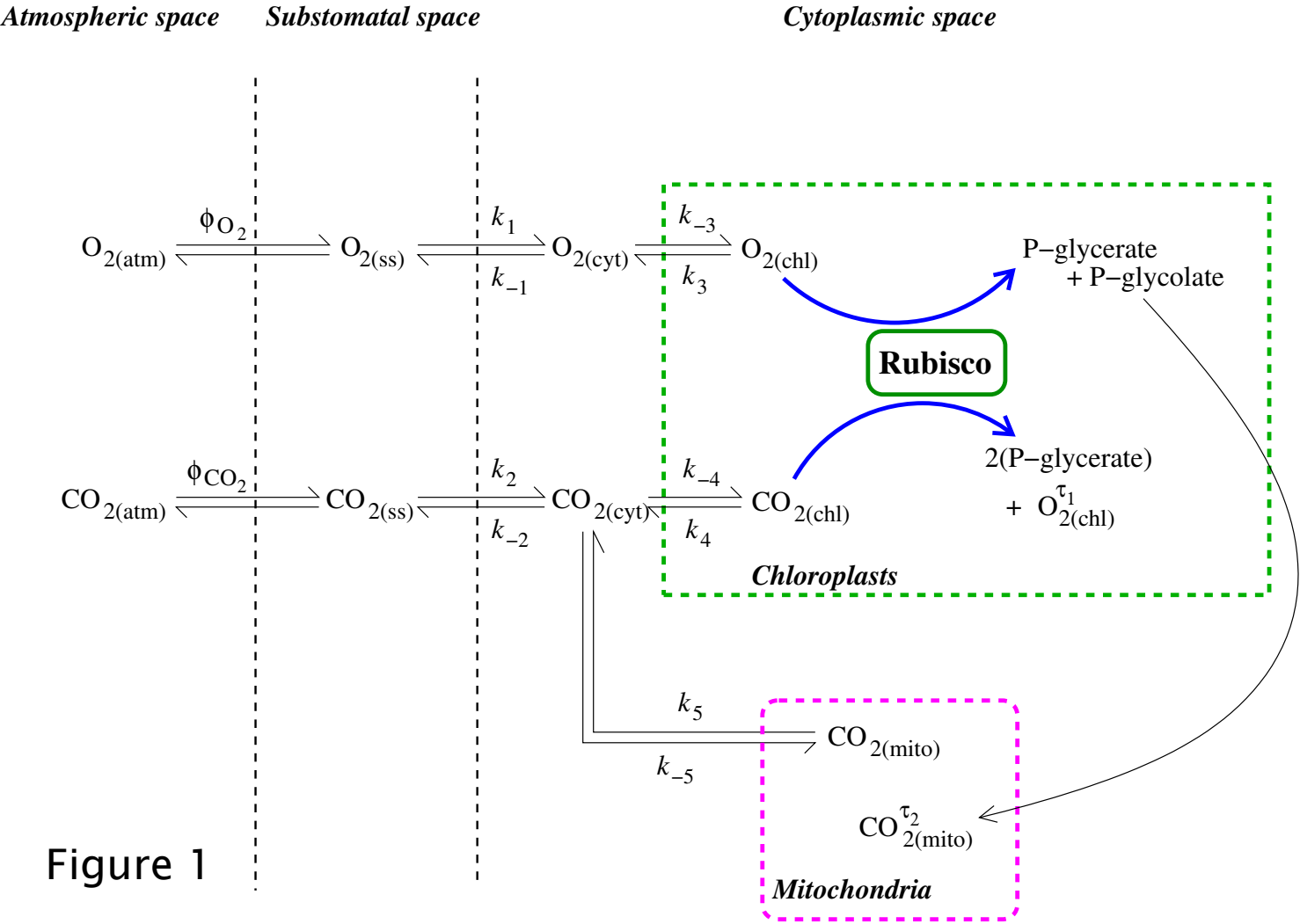
Atmospheric space
Substomatal space
Cytoplasmic space
$O_{2(atm)}$
ϕ_{O_2}
$O_{2(ss)}$
k_1
k_{-1}
$O_{2(cyt)}$
k_{-3}
k_3
$O_{2(chl)}$
P−glycerate
+ P−glycolate
Rubisco
$CO_{2(atm)}$
ϕ_{CO_2}
$CO_{2(ss)}$
k_2
k_{-2}
$CO_{2(cyt)}$
k_{-4}
k_4
$CO_{2(chl)}$
2(P−glycerate)
+ $O^{\tau_1}_{2(chl)}$
Chloroplasts
k_5
k_{-5}
$CO_{2(mito)}$
$CO^{\tau_2}_{2(mito)}$
Mitochondria

Figure 1

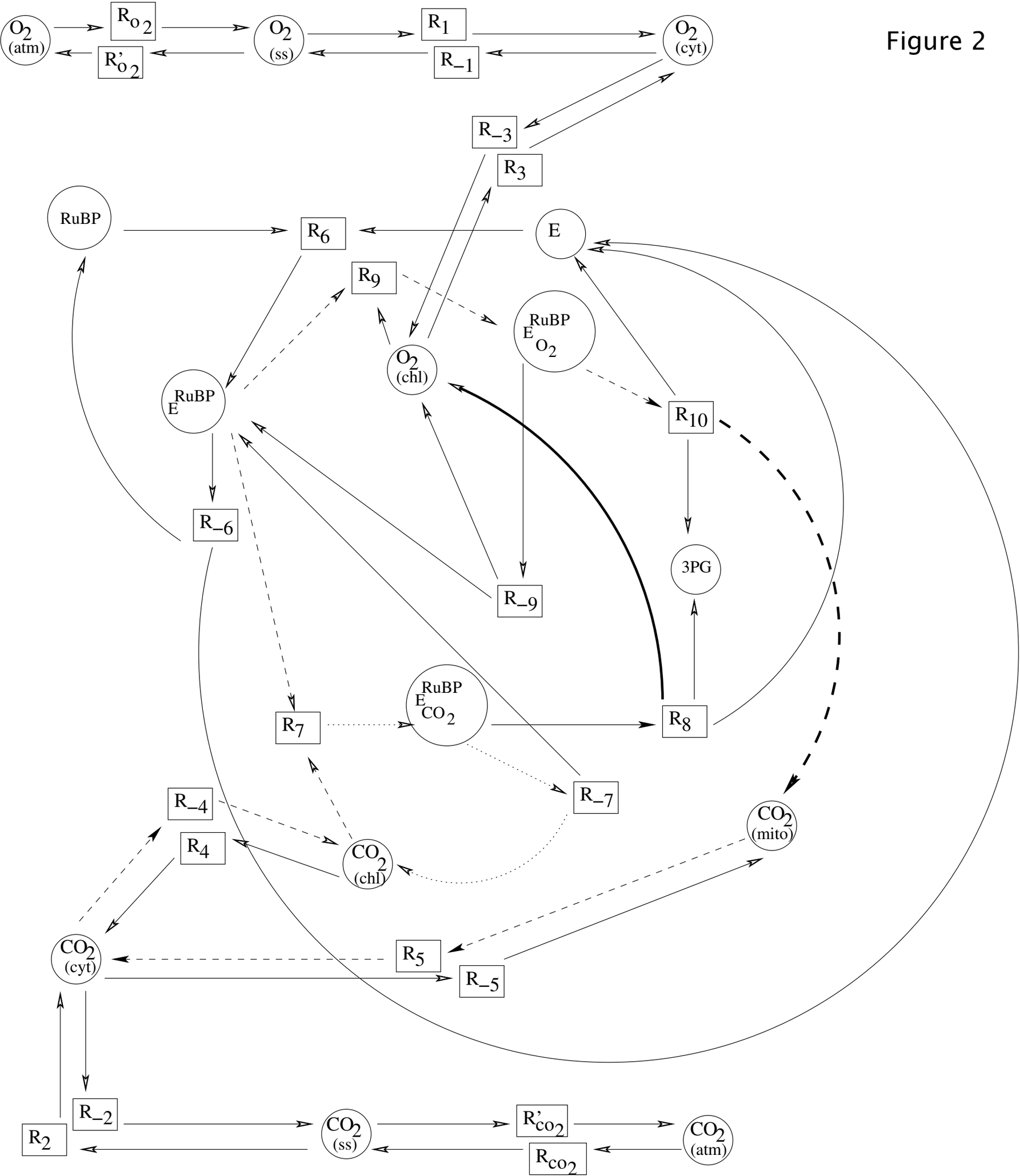
Figure 2
O2 (atm)
Ro 2
O2 (ss)
R1
O2 (cyt)
R'o 2
R–1
R–3
R3
RuBP
R6
E
R9
RuBP E O2
O2 (chl)
RuBP E
R10
R–6
3PG
R–9
RuBP E CO2
R7
R8
R–4
R–7
CO2 (mito)
R4
CO2 (chl)
CO2 (cyt)
R5
R–5
R–2
R2
CO2 (ss)
R'co2
CO2 (atm)
Rco2

Figure 3

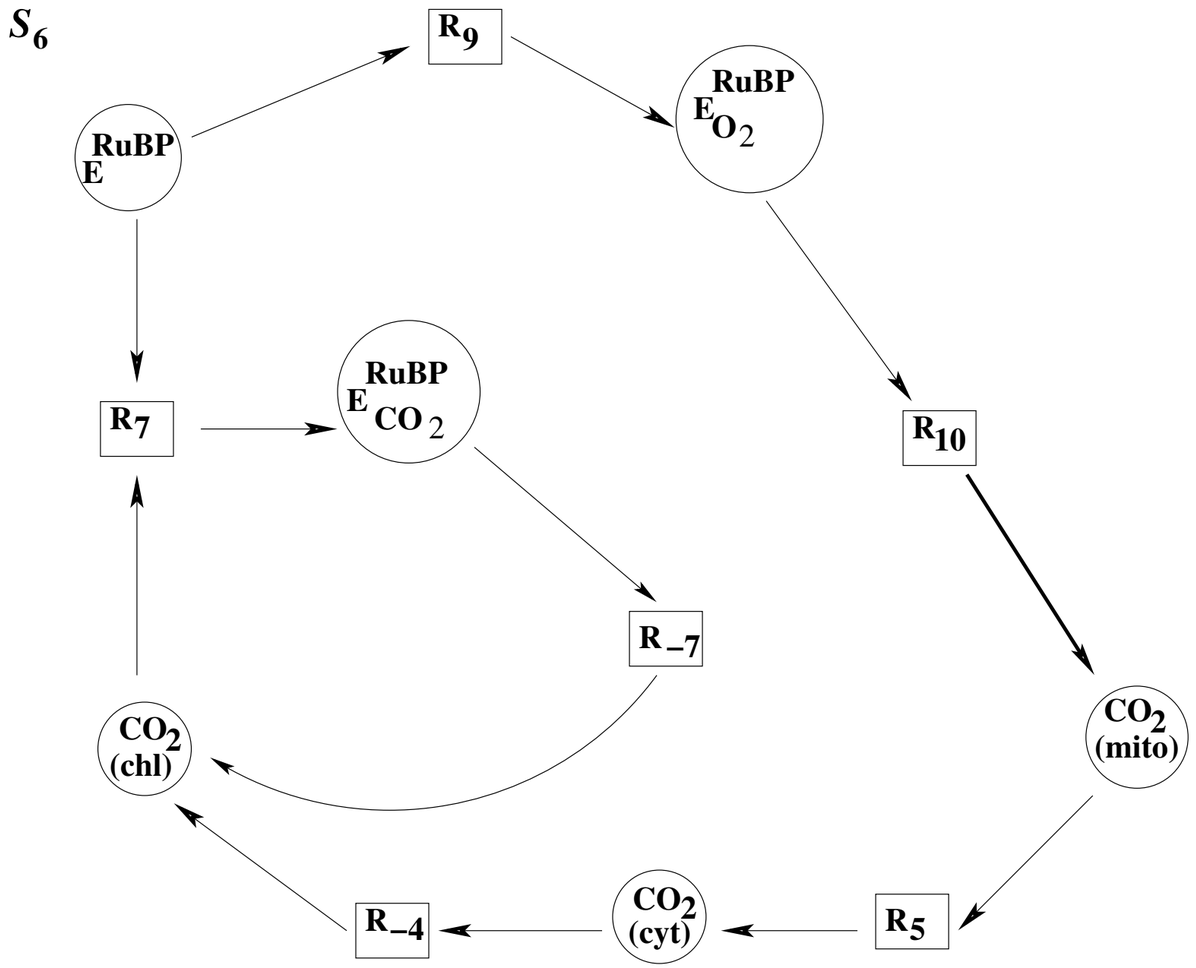
S_6
R9
RuBP E
RuBP E O2
R7
RuBP E CO2
R10
R_7
CO2 (chl)
CO2 (mito)
R_4
CO2 (cyt)
R5

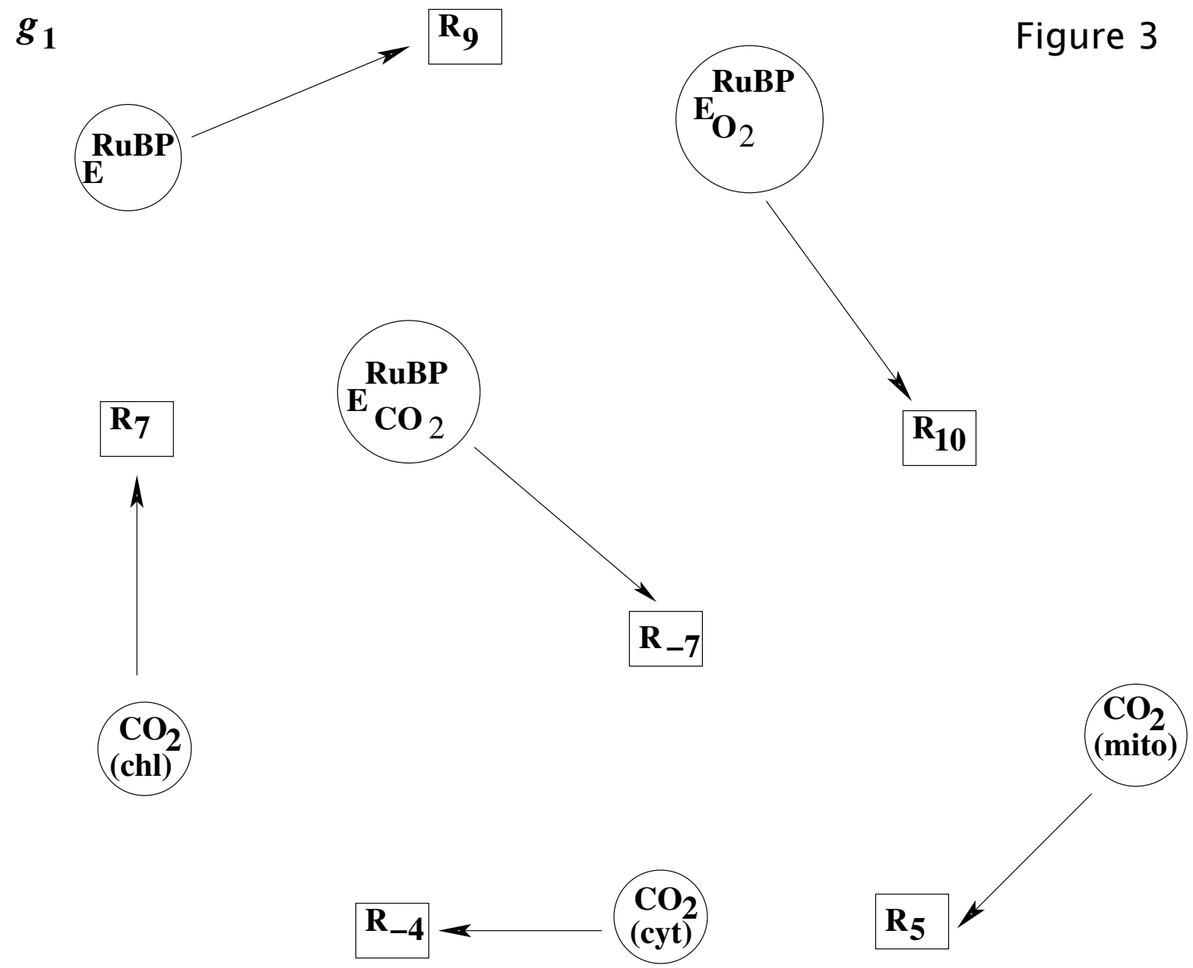
g_1
R9
RuBP E
RuBP E O2
R7
RuBP E CO2
R10
R_7
CO2 (chl)
CO2 (mito)
R_4
CO2 (cyt)
R5

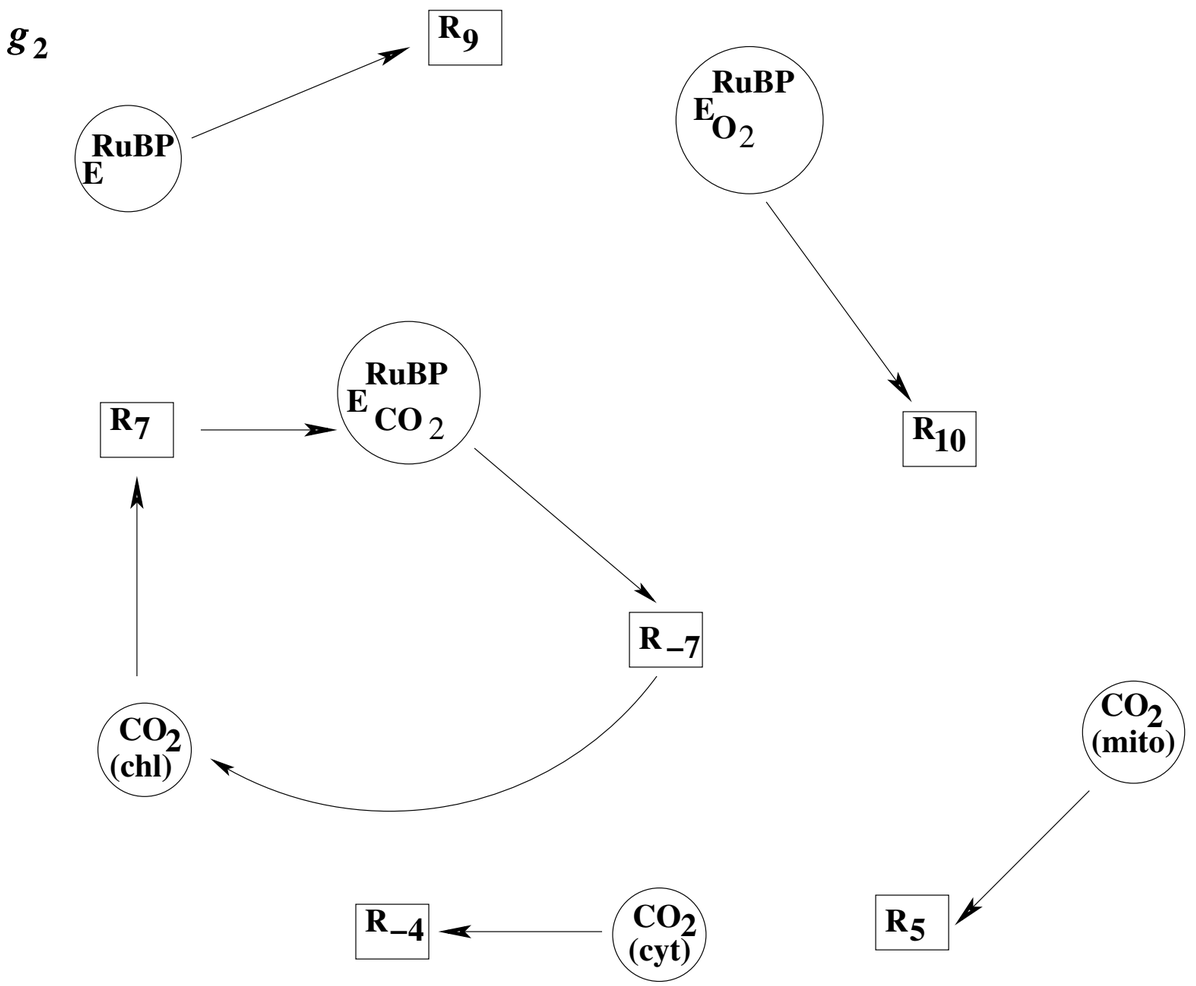
g_2
R9
RuBP E
RuBP E O2
R7
RuBP E CO2
R10
R_7
CO2 (chl)
CO2 (mito)
R_4
CO2 (cyt)
R5

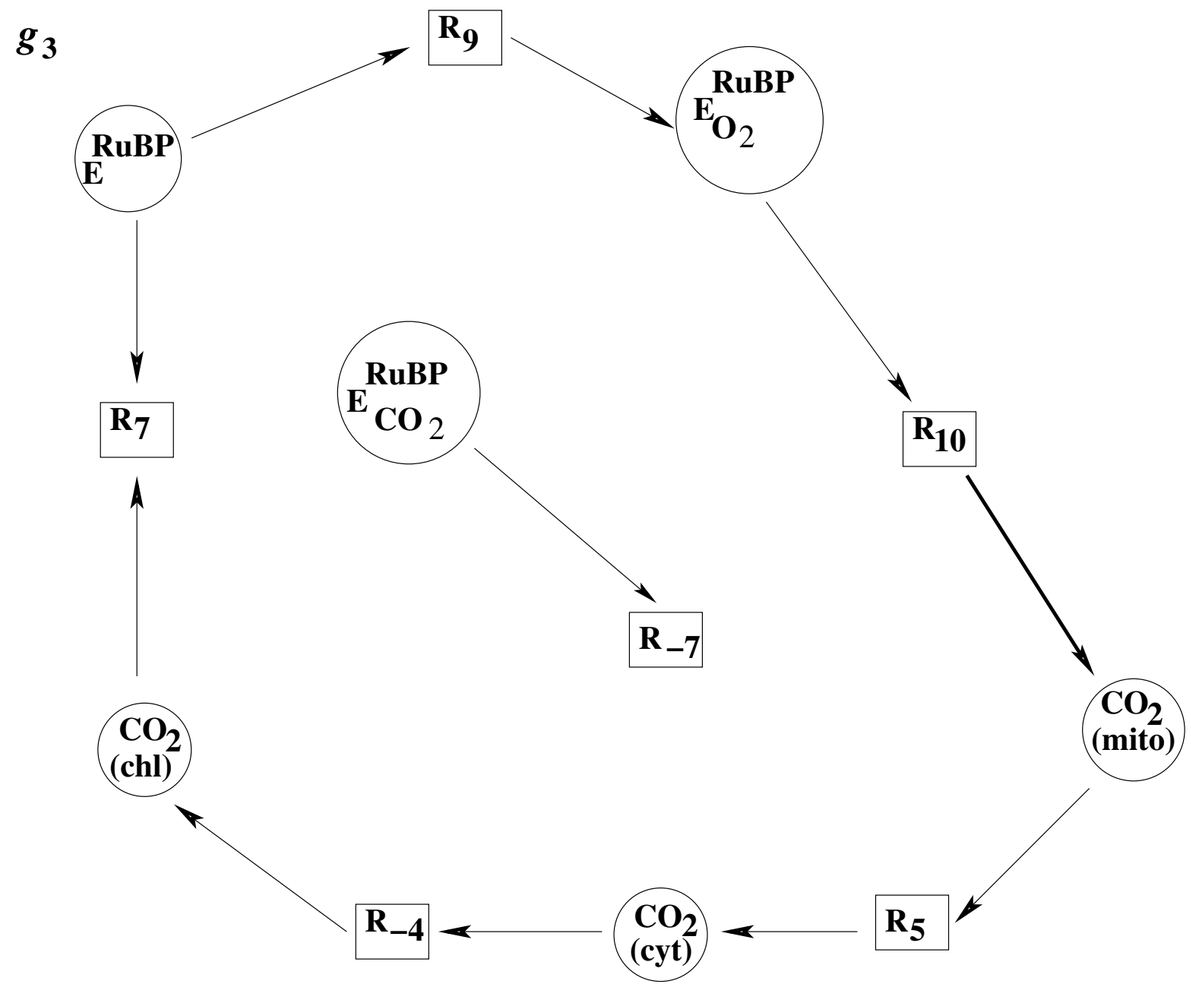
g_3
R9
RuBP E
RuBP E O2
R7
RuBP E CO2
R10
R_7
CO2 (chl)
CO2 (mito)
R_4
CO2 (cyt)
R5

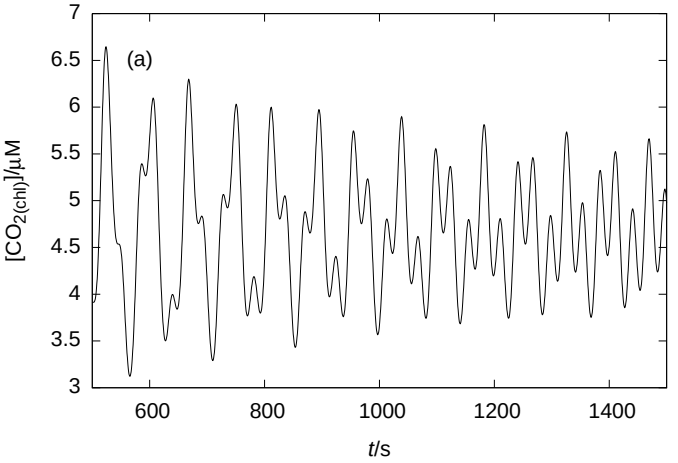
(a)
[CO2(chl)]/μM
t/s
7
6.5
6
5.5
5
4.5
4
3.5
3
600
800
1000
1200
1400

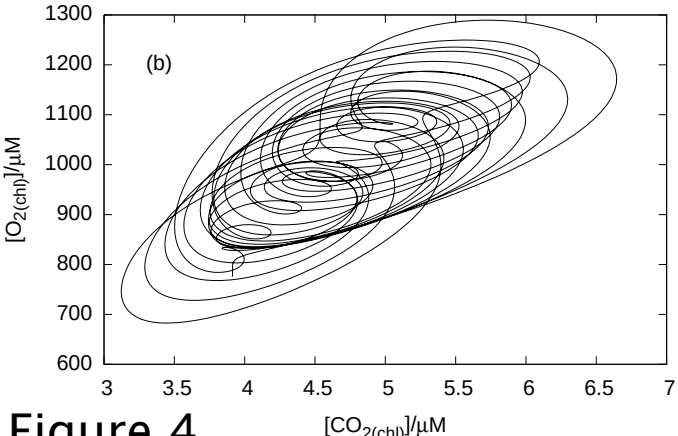
(b)
[O2(chl)]/μM
[CO2(chl)]/μM
1300
1200
1100
1000
900
800
700
600
3
3.5
4
4.5
5
5.5
6
6.5
7

Figure 4

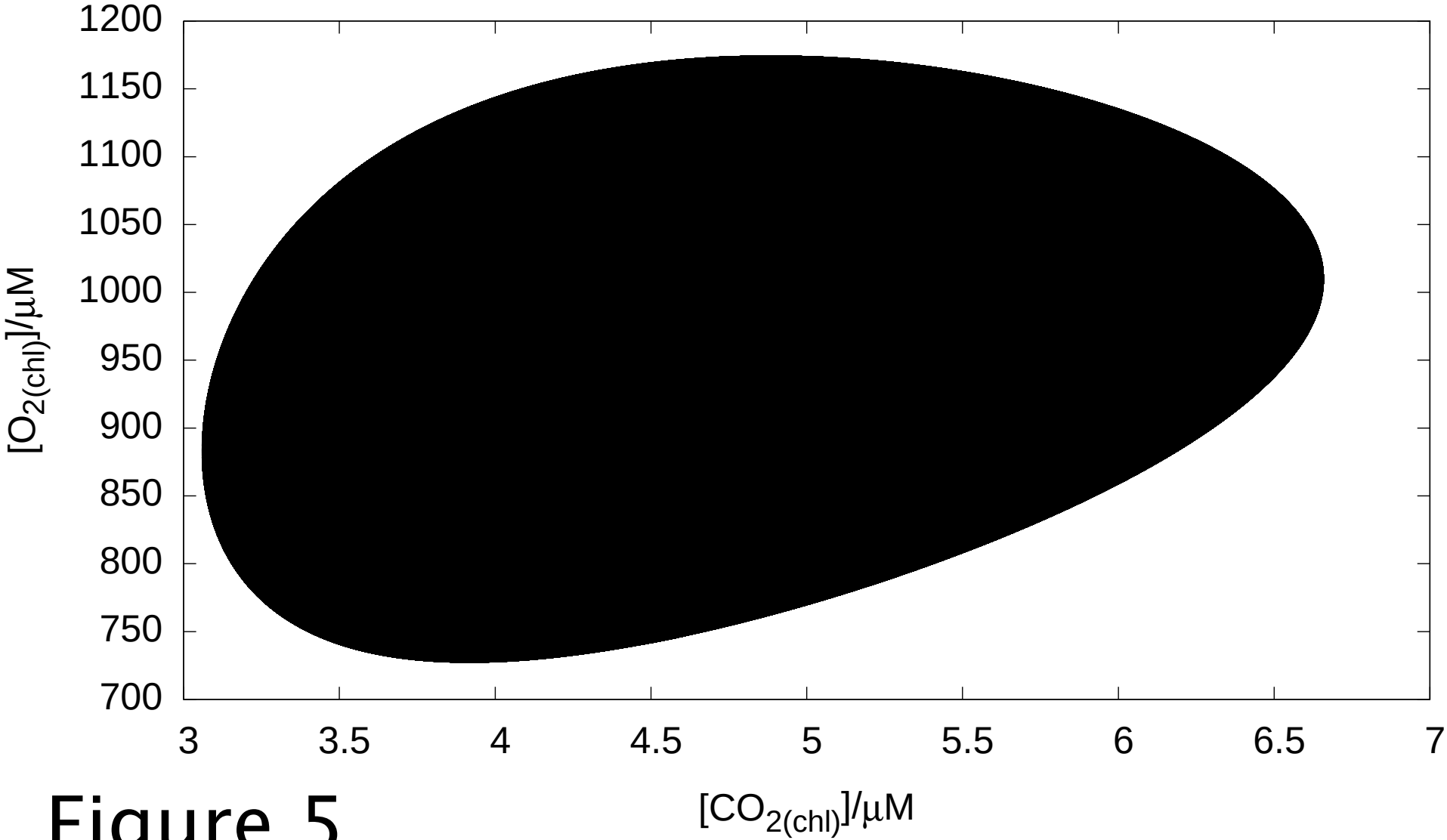

Figure 5